

## Structural Studies of Copper(II)–Amine Terminated Dendrimer Complexes by EXAFS

M. Linh Tran,<sup>†</sup> Lawrence R. Gahan,<sup>‡</sup> and Ian R. Gentle\*

Department of Chemistry, The University of Queensland, Brisbane, Queensland, Australia 4072

Received: November 24, 2003; In Final Form: October 8, 2004

The three-dimensional branched nature of dendritic macromolecules provides many potential sites per molecule for the complexation of metal ions. Therefore, dendrimers may act as hosts for metals with coordination potentially occurring at the periphery, the interior, or both. To understand further the complexation of dendrimers with metal ions EXAFS experiments were carried out. In this work, the interaction of amine-terminated polyamido(amine), PAMAM, dendrimer with copper(II) ions determined by EXAFS is reported. It was found that a model consisting of the copper(II) ion forming five- and six-membered rings by chelating with the primary amine, amide, and tertiary amine nitrogen donors of the PAMAM dendrimer could describe the experimental EXAFS data well. Corroborative evidence for binding to amide nitrogen donors comes from the broadening of NMR resonances of a copper(II)–PAMAM mixture revealing the presence of paramagnetic copper(II) ions at these sites. The significance of the results presented in this paper is that copper(II) ions form complexes within the dendrimer structure and not just at the periphery. The current study may have implications for the use of PAMAM dendrimers as effective ligands in sensing systems.

## Introduction

With their unique properties, dendritic macromolecules have attracted much attention as advanced materials for a variety of applications,<sup>1–3</sup> including contrast agents in magnetic resonance imaging,<sup>4</sup> nanoreactors for particle synthesis,<sup>5</sup> and light harvesting devices,<sup>6</sup> and as metal complexing agents.<sup>6,7</sup> Many of these applications have made use of the interplay between dendrimers and metal ions, with the metal ions present as either structural or nonstructural moieties.<sup>8,9</sup>

One useful property of dendrimers is their three-dimensional branched nature, which provides many potential sites per molecule for the complexation of metal ions. Dendrimers may act as hosts for metals with coordination occurring potentially at the periphery, interior or both. Thus, they may serve as useful polyfunctional ligands and metal ion sequestering agents. It has been reported that it is possible to load commercially available amine-functionalized dendrimers to various metal levels,<sup>10–12</sup> making them potentially useful candidates for metal ion sensor coatings on electrode surfaces.

Research concerning the binding of metal ions to poly-(amidoamine), PAMAM, and poly(propyleneimine), PPI dendrimers has been reported.<sup>3,5,13–18</sup> In particular, the binding of copper(II) ions to amine, hydroxyl, and carboxylate-terminated PAMAM has received considerable attention<sup>8</sup> due to the easily interpretable UV-visible spectra,<sup>10,11</sup> and paramagnetism of the metal ion.<sup>5,16</sup> When copper(II) ions are mixed with either hydroxyl-terminated or amine-terminated PAMAM, the appearance in the UV-visible spectrum of a band at 605 nm, assigned to a d–d transition, and a strong ligand-to-metal charge transfer transition at 300 nm suggest that copper(II) partitions into the dendrimer from the aqueous phase. Crooks and colleagues suggested that for the hydroxyl-terminated dendrimer, copper(II)

binds to the interior two tertiary amines with the other two positions being taken by weakly bound water or amide oxygens.<sup>9</sup>

To assess the roles that primary and tertiary amine nitrogen atoms play in the uptake of copper(II) ions, Tomalia and co-workers used atomic absorption spectroscopy to determine the extent of binding of copper(II) ions with PAMAM and correlated their results to the number of NH<sub>2</sub> terminal groups on each dendrimer. For generation 3–6 (G3–G6) dendrimers, a tetradentate coordination model adequately describes the data. However, it is still uncertain which of the nitrogen donors are involved in coordination.<sup>12</sup>

When EPR spectra of a mixture of copper(II) and the amine-terminated dendrimer were investigated by Ottaviani et al.,<sup>16</sup> the resulting spectra showed a distinct pH dependence. At low pH (<4), where all the nitrogen donor sites are protonated, the signal consisted of predominantly [Cu(H<sub>2</sub>O)<sub>6</sub>]<sup>2+</sup>. In the pH region 4–5 a signal arose from a transient copper(II) species suggesting a Cu–N<sub>2</sub>O<sub>2</sub> chromophore and attributed to a copper(II) species complexed to two primary amine and two water groups in a maximum fraction of about 25%. Finally at higher pH a signal attributed to a Cu–N<sub>4</sub> chromophore appeared. It was postulated that the copper(II) ions responsible for this signal were localized in the internal structure immediately below the external layer (–CH<sub>2</sub>CH<sub>2</sub>NH<sub>2</sub> groups), and the metal ion is bound to two NH<sub>2</sub> and two NR<sub>3</sub> groups. Only at higher pH were the copper(II) ions able to enter the internal PAMAM structure. The authors suggested that the binding abilities of the nitrogen donors to metal ions in the dendrimer follow the trend NH<sub>2</sub> > NR<sub>3</sub> > NHCO.

Despite the EPR, AAS, and UV-visible data presented in the literature, there is still some ambiguity about the binding of dendrimer-chelated copper(II) ions. In this paper a study of the coordination environment of copper(II) ions in a mixture with amine-terminated PAMAM dendrimer, probed using extended X-ray absorption fine structure (EXAFS), is reported.

\* Corresponding author. Telephone: +61-7-3365 4800. Fax: +61-7-3365 4299. E-mail: i.gentle@uq.edu.au.

<sup>†</sup> E-mail: l.tran@chemistry.uq.edu.au

<sup>‡</sup> E-mail: gahan@uq.edu.au

## Experimental Section

**Materials.** Generation 4 (G4) amine-terminated PAMAM (Aldrich; 10% in water or methanol) was diluted to make a  $7.08 \times 10^{-5}$  M solution in distilled water. An aqueous solution of copper(II) nitrate (10 mM) was employed. For the copper(II)–PAMAM mixture, an appropriate aliquot of the 10 mM aqueous solution of copper(II) nitrate was added to PAMAM stock solution to make a 36:1 ratio of copper to dendrimer. The mixture was thoroughly mixed and equilibrated for more than an hour.

**X-ray Absorption Spectroscopy (XAS) Data Collection.** The Cu K-edge X-ray absorption spectra of the copper(II)–PAMAM solution were collected at the Australian National Beamline Facility, on bending magnet beamline 20B at the Photon Factory, Tsukuba, Japan. The ring energy was 2.5 GeV and ring current was 200–400 mA. The Cu K-edge was scanned with radiation from a double Si(111) crystal sagittal focusing monochromator with an energy resolution of  $\Delta E/E = 2 \times 10^{-4}$ . The monochromator was calibrated with copper foil. Data were collected using a 10 multielement array Ge detector (Canberra Industries). The data for the solutions were collected in fluorescence mode with 4–8 scans conducted for each sample.

**EXAFS Data Analysis.** Spectral averaging, background subtraction and model fitting were performed using the XFIT software package.<sup>19</sup> Spectra were averaged and monochromator glitches removed. A second-order polynomial was fitted to the preedge region, extrapolated into the EXAFS region, and subtracted to remove underlying absorbance. A spline polynomial was fitted to the EXAFS region and then subtracted. The data (normalized to an edge jump of 1.0) were converted to  $k$  space, where  $k$  is the photoelectron wavevector  $k = \hbar \sqrt{2m_e(E-E_0)}$ ,  $m_e$  is the electron mass,  $E_0$  is the threshold energy for the  $1s \rightarrow$  continuum transition,  $E$  is the energy of the absorbed X-ray photon, and  $(E - E_0)$  is the energy of the generated photoelectron. Data were multiplied by  $k^3$  to compensate for decreasing EXAFS intensity with increasing photoelectron energy.

The parameters varied during model fitting refinement were as follows: the  $x$ ,  $y$ ,  $z$  coordinates for each scatterer in the model, the Debye–Waller factor,  $\sigma^2$ , of every atom in the model (except the absorbing atom), a scale factor,  $S_0^2$  and  $E_0$ . Values of  $E_0$ ,  $S_0^2$ , the Debye–Waller factors and bond lengths were included in the refinements, and the C–C, C–N and C=O bond lengths were fixed to their typical values.<sup>20</sup>

Determinacy of the models used for EXAFS calculations was checked by method of Binsted et al.,<sup>21</sup> taking into account the applied restraints and constraints. The degree of determinacy of the fit ( $N_i/p$ ) was calculated from the number of independent data points ( $N_i$ ) and parameters ( $p$ ) of the XAFS data set and model, respectively:

$$N_i = \frac{2(\Delta r)(\Delta k)}{\pi} + \sum_i D(N - 2) + 1 \quad (1)$$

where  $\Delta r$  and  $\Delta k$  are the ranges of the FT and XAFS filtered data, respectively, and  $D$  and  $N$  are the number of dimensions (1 for single degree of freedom, 2 for planar groups and 3 for general refinement) and independent atoms per refinement unit, respectively. The final models for each compound refined in this paper were overdetermined.

**NMR Spectroscopy.** Fourier transform  $^{13}\text{C}$  and  $^1\text{H}$  NMR spectra were recorded with a Bruker AC 400 MHz NMR spectrometer with an internal lock.  $\text{CD}_3\text{OD}$  or  $\text{D}_2\text{O}$  were used

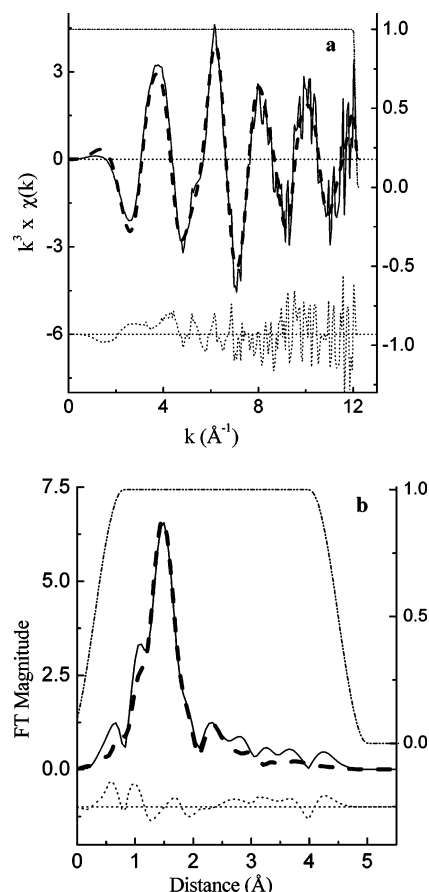


**Figure 1.** (a) EXAFS and (b) FT magnitude of the EXAFS for five coordinate copper using a model featured in Figure 2 ((—) observed and (---) calculated from the refined model using MS analysis).

as solvents. Samples of 10% PAMAM in methanol solution were saturated with copper(II) nitrate solution (10 mM).

**TEM.** The TEM study was performed with a JEOL 1010 electron microscope at 80 kV. The substrates used were carbon-coated Formvar nickel grids and were viewed beforehand for any external contamination. A glow discharge was applied to all substrates before experiments began.

To a 1 mM solution of PAMAM in methanol (prepared from a 10% PAMAM stock solution) was added an appropriate aliquot of 10 mM solution of copper(II) nitrate in water to prepare a mixture in 36:1 metal ion-to-dendrimer ratio. The mixture was allowed to equilibrate for 20 min.

## Results and Discussion

**Copper(II) and PAMAM Dendrimers.** Upon mixing the copper(II) nitrate solution with the PAMAM dendrimer solution, the mixture turned a purple-blue color associated with the formation of copper(II)–amine complexes. Figure 1 shows the Cu K edge EXAFS spectrum for the mixture of copper(II)–PAMAM, along with the corresponding Fourier transform. From the spectra, it is evident that the total  $\chi(k)$  signal is dominated by the first shell contributions with the inclusion of the additional signals to reproduce the high-frequency pattern of the experimental spectra.

In the first instance, single scattering (SS) analyses<sup>22</sup> of the EXAFS data (Supporting Information) revealed that the first coordination shell consisted of four or five N atoms at a distance of 1.98 Å and one O or one N atom at a distance of 2.28 Å. On the basis of this initial analysis various models, which included carbon and oxygen atoms of the dendrimer framework, were

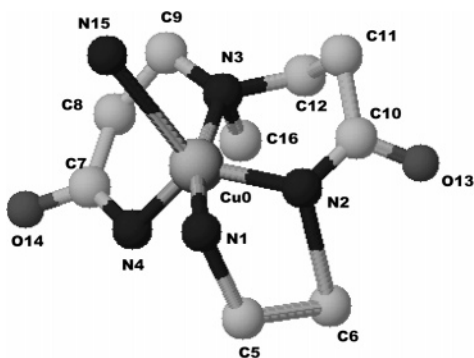


**Figure 2.** Model obtained after refinement for 36:1 copper(II):PAMAM dendrimer mixture.

**TABLE 1: Summary of EXAFS Modeling Results for the Model in Figure 2**

parameters	values <sup>a</sup>
<i>R</i> , %	19.87
$\Delta E_0$ , eV	-11.1
<i>S</i> <sub>0</sub> <sup>2</sup>	0.91
<i>N</i> / <i>p</i> (determinancy)	1.16
<i>r</i> (Cu–N1), Å	1.98(2)
<i>r</i> (Cu–N2), Å	1.98(2)
<i>r</i> (Cu–N3), Å	1.98(2)
<i>r</i> (Cu–N4), Å	1.98(2)
<i>r</i> (Cu–N15), Å	2.84(2)
$\sigma^2_{15}$ , Å <sup>2</sup>	0.0042(0)
$\sigma^2_{21}$ , Å <sup>2</sup>	0.0042(0)
$\sigma^2_{31}$ , Å <sup>2</sup>	0.0042(0)
$\sigma^2_{41}$ , Å <sup>2</sup>	0.0042(0)
$\sigma^2_{15}$ , Å <sup>2</sup>	0.0105(0)

<sup>a</sup> Estimated errors for  $\sigma^2$ , obtained from Monte Carlo method was less than  $10^{-4}$ .

constructed and applied to the EXAFS data, using multiple scattering (MS) analysis.<sup>23</sup> After several trial structures were tested for their ability to reproduce the EXAFS data, it was found that a model consisting of copper(II) ions surrounded by three chelate rings with four nitrogen donors in close proximity and a further N or O donor at a longer distance to complete the coordination sphere, produced a good fit. The model, which gave a goodness of fit parameter of 19.87%, is shown in Figure 2. To form the five and six-membered chelate rings one primary amine (N1) nitrogen atom, two amide (N2 and N4) nitrogen atoms, and one tertiary amine (N3) nitrogen atom were used. An axial atom (N15) is located at a distance of 2.84(2) Å from the copper center. It is also worth noting that, although a N atom was placed in the axial position, it could equally be an O atom as the two elements have similar atomic weights, sizes, and electronic configurations and hence similar backscattering functions. The shape of the Fourier transform is reminiscent of that obtained for copper(II) complexes with one or two axial donor ligands.<sup>24–26</sup> The source of this axial group may be from weakly bound atoms of the dendrimer or surrounding solvent molecules. The other four Cu–N bond distances were restrained to 1.98(2) Å (as indicated by the single scattering analysis) so that the fits were overdetermined. Table 1 shows the resulting parameters obtained after the refinement process using this model.

The extracted Cu–N bond distance agrees with the Cu–N value reported in a recent publication on copper(II)–PAMAM complexes.<sup>27</sup> Cu–N distances between 1.98 and 2.07 Å have been reported for complexes containing copper amine/amine bonds,<sup>28–33</sup> while crystal structures containing both copper–amide nitrogen and copper–primary amine nitrogen bonds reported in the literature have bond lengths between 1.92 and

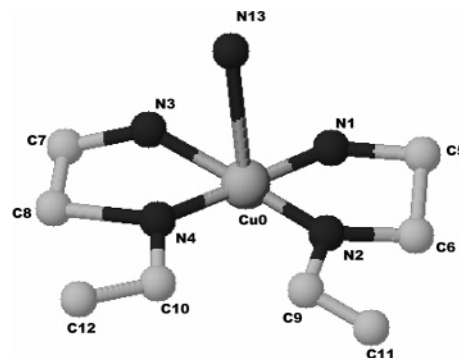


**Figure 3.** Five-coordinate copper–PAMAM model using two primary amines (N1 and N3) and two amide nitrogens (N2 and N4) for coordination with an additional apical nitrogen (N13).

1.99 Å.<sup>28,34–36</sup> Solution EXAFS studies of copper(II)–amine,<sup>31</sup> and copper–PPI dendrimer<sup>24</sup> complexes have produced Cu–N bond distances of 2.02 and 2.03 Å, respectively. Although desirable, it was not possible to extract meaningful multiple Cu–N bond distances under the experimental conditions used here. Nonetheless the value of 1.98 Å is a reasonable value for such bond types.

The Debye–Waller factor for the axial donor atom (N15) was high in comparison to the other N atoms as expected,<sup>37</sup> reflecting the different strength of interactions along the axial direction and therefore the greater fluctuations in the position of this donor. Contributions from scattering by the outer carbons (C5, C7, C9, and C16) and oxygen atom (O14) in scattering pathways were important as evidenced by the high percentage contribution (~20%) of paths in these atoms, relative to the most important path (Supporting Information). It is worth stressing that the model obtained cannot be assumed to be the only species present in the solution sample. Uncertainty in the Debye–Waller factors of the outer atoms, carbon and oxygen, is expected as these systems have a high degree of structural disorder.

An alternate model of interest, which was investigated, was one where two amido amine and two primary amine nitrogen donors were involved in coordination with the copper(II) ion as shown in Figure 3. It was found that when modeling the EXAFS and corresponding FT data, the Debye–Waller factors of most of the atoms including two of the nitrogen atoms reached their limits (Supporting Information). Thus, the model was not adequate to represent the species in solution. Participation of the tertiary amine groups in the uptake of copper(II) by dendrimer molecules has been probed by Diallo et al.<sup>27</sup> They found that by modifying G4 amine-terminated PAMAM dendrimers with terminal acetamide (NH–COCH<sub>3</sub>) groups no uptake was observed at low pH, whereas at neutral and basic pHs uptake of copper(II) ions occurs when the tertiary amine groups are deprotonated.<sup>27</sup>

To improve the reliability of the MS structure, it would be of use to conduct further EXAFS experiments to higher *k* values, higher concentrations of copper(II) and/or with the use of a more intense beamline. It is also of value to use another technique to provide supporting evidence for the model proposed, and hence NMR experiments, as described below, were undertaken to probe the environment around the copper(II) ions.

The significant result of the analysis in the paper is that in order to achieve the five coordinate arrangement outlined in the EXAFS analysis there needs to be movement of the copper(II) ions into the dendrimer structure. In particular, involvement of the amide nitrogen of the PAMAM dendrimer



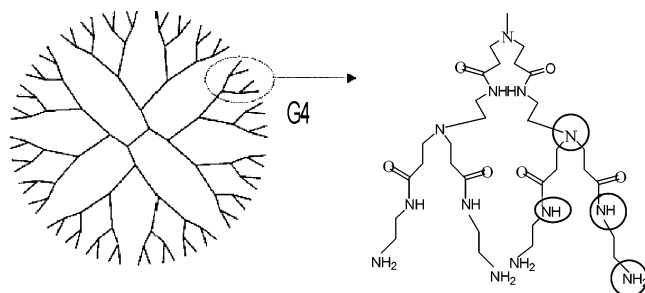


**Figure 4.** Schematic for the location of potential donor groups used to chelate with the copper(II) ions.

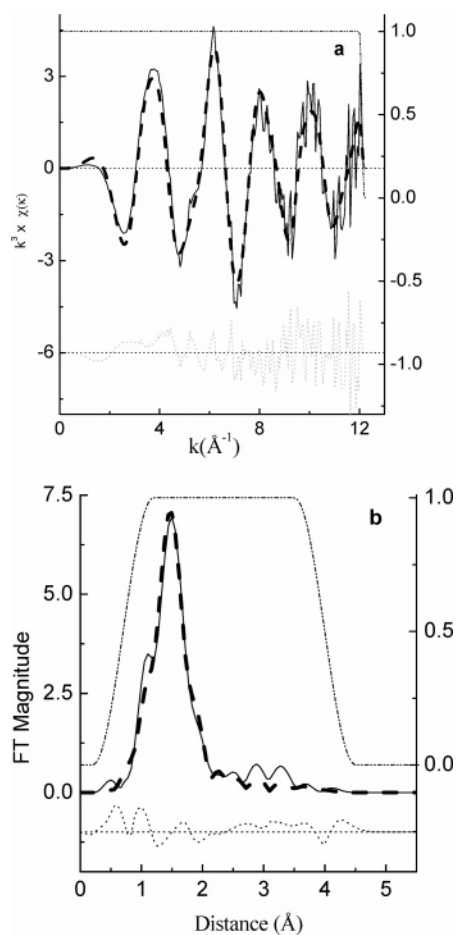


**Figure 5.** (a) EXAFS and (b) FT magnitude of the EXAFS of copper(II) nitrate for five coordinate copper using four oxygen scatterers in the equatorial plane and one axial oxygen scatterer ((—) observed and (---) calculated from refined model).

internal structure is suggested by this study. The possible positions of the donor groups are shown in Figure 4.

**Copper(II) Nitrate.** To verify that the EXAFS signals from the copper(II)–dendrimer mixture were not a result of only the hydrated copper(II) ion in solution, the transmission EXAFS spectrum of 10 mM copper(II) nitrate was acquired. It was found that the theoretical fit of a two shell model with the copper atom surrounded by four oxygen scatterers in one shell and one oxygen scatterer in another shell surrounding the copper atom at distances of 1.960(2) and 2.247(5) Å with corresponding Debye–Waller factors of 0.0047(2) and 0.0129(13), respectively, could adequately reproduce the experimental data. Figure 5 shows the fitted EXAFS and corresponding Fourier transform for the copper(II) nitrate salt solution.

In contrast, application of the model used for copper(II) nitrate EXAFS spectrum to the data obtained for the copper(II)–

**TABLE 2:**  $^{13}\text{C}$  NMR Assignments of PAMAM (10% in MeOH) (Solvent =  $\text{CD}_3\text{OD}$ )

peaks/ppm	assignment	lit. <sup>38,39</sup> /ppm
175.12	–CONH	178.0, 177.4
174.68		
174.59		
53.53	$\text{NHCH}_2\text{CH}_2\text{N}$	52.3
51.15	$\text{CH}_2\text{CH}_2\text{CONHCH}_2\text{CH}_2\text{NH}_2$	50.1
43.06	$\text{CONHCH}_2\text{CH}_2\text{NH}_2$	42.7
42.11	– $\text{CH}_2\text{NH}_2$	40.9
38.63	$\text{NHCH}_2\text{CH}_2\text{N}$	37.8
34.82	$\text{CH}_2\text{CONHCH}_2\text{CH}_2\text{NH}_2$	33.9
33.29		33.7

PAMAM mixture did not give a good fit. Also it was obvious from comparing FT for both copper(II) nitrate alone and the copper(II)–PAMAM mixture that the post 2 Å regions were different for both solution types. The results suggest that the EXAFS data for copper(II)–PAMAM mixture were not solely due to the hydrated copper(II) ion species.

$^{13}\text{C}$  and  $^1\text{H}$  NMR experiments were conducted to determine whether the coordination of the copper(II) was occurring near the amide nitrogen atoms, as suggested by the model proposed for the EXAFS data in Figure 2. The presence of nearby paramagnetic species, such as copper(II), would be expected to induce broadening of resonances in proximity to the paramagnetic center. It would therefore be possible to probe the binding site of the copper(II) ion within the dendritic molecule.

The  $^{13}\text{C}$  NMR spectrum of a methanolic solution of PAMAM consists of peaks in the regions 180–160 ppm and 65–20 ppm (Figure 6a). The assignments of the spectrum were based on previous literature reports<sup>38,39</sup> and are tabulated in Table 2.

Upon addition of copper(II) to PAMAM solution broadening of the carbonyl signal from the amide group is observed (Figure 6b), suggesting that the copper(II) ion was coordinated adjacent to these amide sites. In addition the signals at 43–42 ppm collapsed after addition of copper(II) to the dendrimer solution, a result which could be attributed to the presence of copper(II) near the amide nitrogen and primary amine groups. In another  $^{13}\text{C}$  NMR experiment conducted with  $\text{D}_2\text{O}$  (Supporting Information) there was a slight shifting of the peak associated with the  $\text{NCH}_2\text{CH}_2\text{CONHCH}_2\text{CH}_2\text{NH}_2$  carbon at ~50 ppm after addition of copper(II) into the dendrimer solution, which may indicate the influence of the metal ion near that tertiary nitrogen amine site. The other resonances in Figure 6b retained their narrow line width despite addition of the paramagnetic ion to the dendrimer solution.

Comparison of the  $^1\text{H}$  NMR spectra of copper(II)–dendrimer complexes and the free dendrimer ligand in  $\text{D}_2\text{O}$  revealed broadening of the triplet signal at 2.52 ppm, associated with the  $\text{CH}_2$  unit attached to the primary amine groups (Figure 7), again supporting the association of copper(II) ions with primary amine groups.

The NMR data lends support to the proposed binding arrangement of the PAMAM dendrimer around the copper(II) ion site proposed from the EXAFS data. In particular, incorporation of the metal ion within the interior structure of the dendrimer is confirmed. The results suggest the copper(II) ions bind to all three types of nitrogen donors of the dendrimer framework, not just the primary and tertiary amine nitrogen groups as suggested by the previous literature.<sup>12,16</sup> In addition, copper(II) ions are capable of effectively competing with amide hydrogens to enter the internal structure of the dendrimer even in the absence of strong base. By chelating to the copper(II) ion in the manner shown in Figure 2, five- and six-membered rings are formed, in contrast to the larger rings that would occur

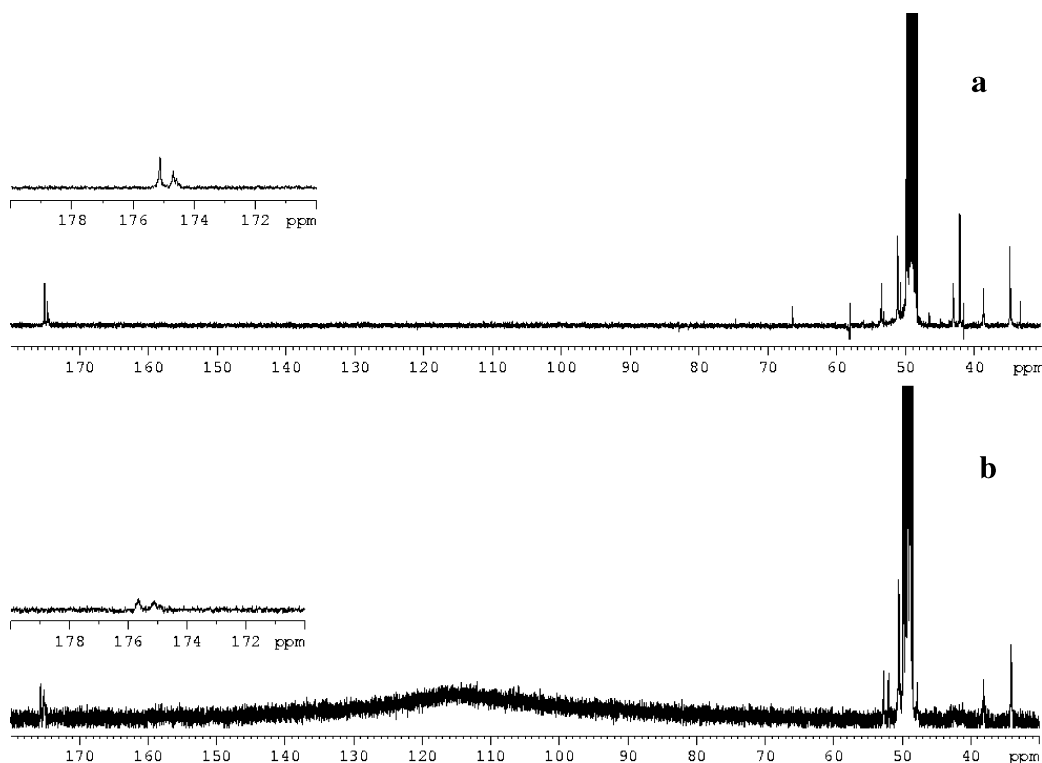


**Figure 6.**  $^{13}\text{C}$  NMR spectra of (a) PAMAM in  $\text{CD}_3\text{OD}$  and (b) copper(II) with PAMAM.

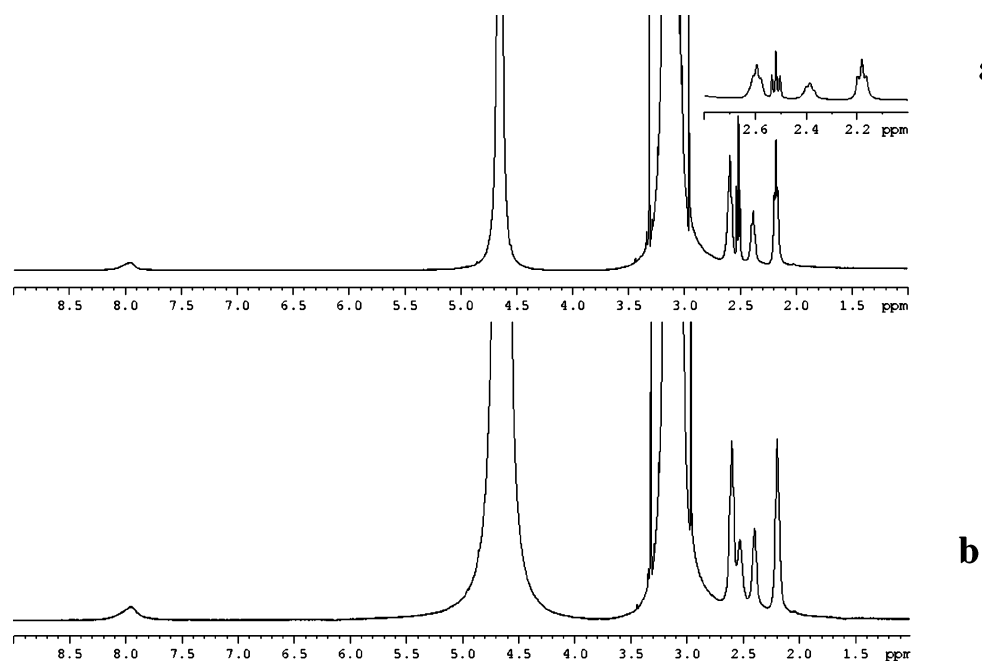


**Figure 7.**  $^1\text{H}$  NMR spectra of (a) PAMAM alone and (b) copper(II) and PAMAM in  $\text{D}_2\text{O}$ .

for the tetradentate model reported previously.<sup>12,16</sup> In the literature model<sup>12,16</sup> two primary and two tertiary nitrogens would be required to participate in large, weaker nine-membered rings with the copper(II) ion, thus reducing the influence of the chelate effect,<sup>40</sup> compared with the more stable five and six-membered rings shown in Figure 2.<sup>12,16</sup> The stability of complexes, in general, decreases with increasing ring size.<sup>40</sup>

Finally, examination of copper(II)-loaded dendrimer particles with TEM (Figure 8) showed that the metal ion–dendrimer composites are spherically uniform in shape with a diameter of  $7.4 \pm 1.3$  nm and have an even density distribution across the whole particle. TEM inspection of the 1 mM PAMAM dendrimer solution with no added copper(II), using a staining

reagent, reveals particles of dimensions  $6.1 \pm 1.7$  nm (Figure 8), within the range of previous dendrimer size measurements.<sup>9</sup> It is also notable that there was a greater electron density in the copper(II)-loaded particles than in the stained dendrimer particles supporting the hypothesis of incorporation of copper ions into the dendrimer particles and formation of copper complexes.

**Comments on Cu XANES Region.** Figure 9 shows the XANES region for copper(II) nitrate and copper(II)–PAMAM solutions. It is known that a sharp preedge feature at 8984 eV is present in the absorption spectra of copper(I) species, but not for complexes of copper(II).<sup>41</sup> Copper(II) compounds do not show edge absorption features below 8985 eV, except for a well separated weak 8978 eV absorption feature, which is

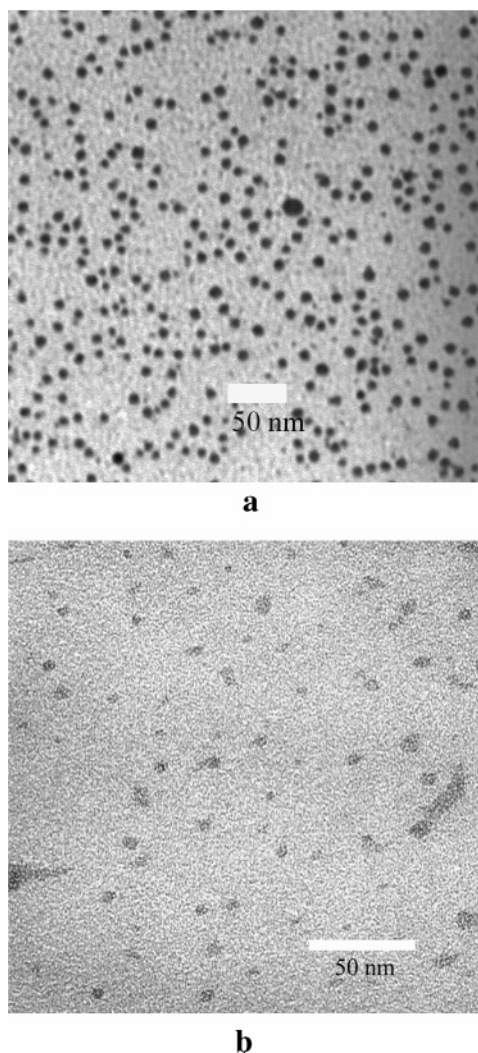


**Figure 8.** (a) 36:1 copper(II): PAMAM mixture. (b) Generation 4  $\text{NH}_2$ -terminated PAMAM dendrimer.

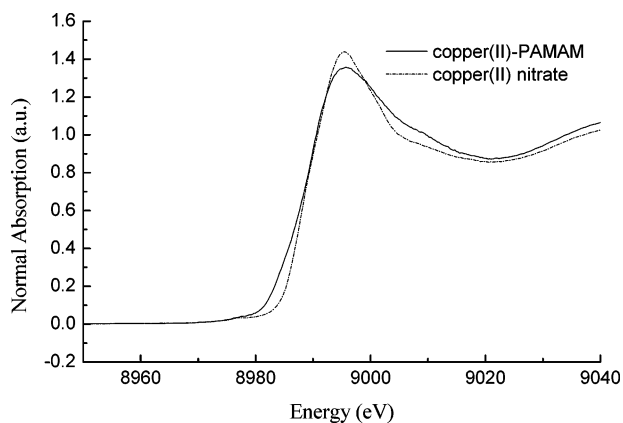


**Figure 9.** XANES region of copper(II) nitrate and mixture of copper(II) with PAMAM.

the  $1s-3d$  transition.<sup>41,42</sup> The intensity of the 8978 eV peak increases with increasing tetrahedral distortion, due to Cu  $4p-3d$  mixing.<sup>41</sup>

In the XANES of copper(II)–PAMAM mixture an additional transition at 8986 eV is observed and assigned as the  $1s-4p_\pi$  plus ligand to copper(II) charge-transfer shakedown.<sup>42</sup> The low intensity of the 8986 eV feature for the copper(II)–PAMAM XANES region suggests a distortion of the copper(II) site away

from tetragonal symmetry.<sup>42</sup> The XANES data is consistent with the earlier model proposed for the analysis of the EXAFS data.

## Conclusions

EXAFS data for copper(II)–PAMAM solutions were fitted with acceptable parameters using a model in which primary amine, amide and tertiary amine nitrogen atoms are involved in bonding with the copper(II) ion to form five- and six-membered rings. This result implies that copper(II) forms complexes within the PAMAM dendrimer structure and not just at the periphery. The presence of nearby paramagnetic copper(II) ions resulted in broadening of the  $^{13}\text{C}$  and  $^1\text{H}$  NMR signals associated with  $-\text{CH}_2\text{NH}_2$ ,  $\text{CONHCH}_2\text{CH}_2\text{NH}_2$ , and  $\text{CONH}$  moieties, indicating binding to these nitrogen sites. TEM images of the copper(II)–PAMAM mixture revealed particles of spherical structure with comparable diameters to those reported for the radius of gyration of the dendrimer ligand. The current study shows that generation 4 amine-terminated PAMAM dendrimer effectively interacts with copper(II) ions and therefore would serve as a suitable candidate for receptors in a sensing system.

**Acknowledgment.** This work was performed at the Australian National Beamline Facility with support from the Australian Synchrotron Research Program, which is funded by the Commonwealth of Australia under the Major National Research Facilities Program. The authors are grateful for the assistance of Dr Garry Foran with the EXAFS measurements.

**Supporting Information Available:** Tables of single scattering fits to the copper and PAMAM (36:1) EXAFS data, EXAFS parameters obtained after fitting the data using the model shown in Figure 2, summary of the conditions, restraints, and constraints applied to the simulations of the XAFS spectra, summary of the major multiple-scattering pathways required to model the EXAFS spectrum for 36:1, and EXAFS parameters obtained after fitting the data using the model shown in Figure 3 and a figure showing the  $^{13}\text{C}$  NMR spectra of  $\text{Cu}^{2+}$  with PAMAM and PAMAM in  $\text{D}_2\text{O}$ . This material is available free of charge via the Internet at <http://pubs.acs.org>.

## References and Notes

- (1) Bosman, A. W.; Janssen, H. M.; Meijer, E. W. *Chem. Rev.* **1999**, 99, 1665–1688.
- (2) Tomalia, D. A.; Durst, H. D. *Top. Curr. Chem.* **1993**, 165, 193–313.
- (3) Zeng, F. W.; Zimmerman, S. C. *Chem. Rev.* **1997**, 97, 1681–1712.
- (4) Fischer, M.; Vogtle, F. *Angew. Chem., Int. Ed.* **1999**, 38, 885–905.
- (5) Ottaviani, M. F.; Valluzzi, R.; Balogh, L. *Macromolecules* **2002**, 35, 5105–5115.
- (6) Vogtle, F.; Gestermann, S.; Hesse, R.; Schwierz, H.; Windisch, B. *Prog. Polym. Sci.* **2000**, 25, 987–1041.
- (7) Sun, L.; Crooks, R. M. *J. Phys. Chem. B* **2002**, 106, 5864–5872.
- (8) Crooks, R. M.; Lemon, B. I., III; Sun, L.; Yeung, L. K.; Zhao, M. *Top. Curr. Chem.* **2001**, 212, 81–135.
- (9) Crooks, R. M.; Zhao, M.; Sun, L.; Chechik, V.; Yeung, L. K. *Acc. Chem. Res.* **2001**, 34, 181–190.
- (10) Zhao, M.; Sun, L.; Crooks, R. M. *J. Am. Chem. Soc.* **1998**, 120, 4877–4878.
- (11) Balogh, L.; Tomalia, D. A. *J. Am. Chem. Soc.* **1998**, 120, 7355–7356.
- (12) Diallo, M. S.; Balogh, L.; Shafagati, A.; Johnson, J. H., Jr.; Goddard, W. A. III; Tomalia, D. A. *Environ. Sci. Technol.* **1999**, 33, 820–824.
- (13) Balogh, L.; Valluzzi, R.; Laverdure, K. S.; Gido, S. P.; Hagnauer, G. L.; Tomalia, D. A. *J. Nanopart. Res.* **1999**, 1, 353–368.
- (14) Zhao, M. Q.; Crooks, R. M. *Chem. Mater.* **1999**, 11, 3379–3385.
- (15) Ottaviani, M. F.; Montalti, F.; Romanelli, M.; Turro, N. J.; Tomalia, D. A. *J. Phys. Chem.* **1996**, 100, 11033–11042.

- (16) Ottaviani, M. F.; Montalti, F.; Turro, N. J.; Tomalia, D. A. *J. Phys. Chem. B* **1997**, *101*, 158–166.
- (17) Esumi, K.; Suzuki, A.; Yamahira, A.; Torigoe, K. *Langmuir* **2000**, *16*, 2604–2608.
- (18) Bosman, A. W.; Schenning, A.; Janssen, R. A. J.; Meijer, E. W. *Chem. Ber./Recl.* **1997**, *130*, 725–728.
- (19) Ellis, P. J.; Freeman, H. C. *J. Synchrotron Radiat.* **1995**, *2*, 190–195.
- (20) *CRC handbook of chemistry and physics*, 58th ed.; CRC Press: Boca Raton, FL, 1977–1978.
- (21) Binsted, N.; Strange, R. W.; Hasnain, S. S. *Biochemistry* **1992**, *31*, 12117–12125.
- (22) Mustre de Leon, J.; Rehr, J. J.; Zabinsky, S. I.; Albers, R. C. *Phys. Rev. B: Condens. Matter* **1991**, *44*, 4146–4156.
- (23) Rehr, J. J.; Mustre de Leon, J.; Zabinsky, S. I.; Albers, R. C. *J. Am. Chem. Soc.* **1991**, *113*, 5135–5140.
- (24) Floriano, P. N.; Noble, C. O.; Schoonmaker, J. M.; Poliakoff, E. D.; McCarley, R. L. *J. Am. Chem. Soc.* **2001**, *123*, 10545–10553.
- (25) D'Angelo, P.; Bottari, E.; Festa, M. R.; Nolting, H. F.; Pavel, N. V. *J. Phys. Chem. B* **1998**, *102*, 3114–3122.
- (26) D'Angelo, P.; Bottari, E.; Festa, M. R.; Nolting, H. F.; Pavel, N. V. *J. Chem. Phys.* **1997**, *107*, 2807–2812.
- (27) Diallo, M. S.; Christie, S.; Swaminathan, P.; Balogh, L.; Shi, X.; Um, W.; Papelis, C.; Goddard, W. A., III; Johnson, J. H., Jr. *Langmuir* **2004**, *20*, 2640–2651.
- (28) Brooker, S.; Dunbar, G. S.; Plieger, P. G. *Inorg. Chim. Acta* **2000**, *304*, 204–209.
- (29) Valli, M.; Matsuo, S.; Wakita, H.; Yamaguchi, T.; Nomura, M. *Inorg. Chem.* **1996**, *35*, 5642–5645.
- (30) Kelly, S. D.; Kemner, K. M.; Fryxell, G. E.; Liu, J.; Mattigod, S. V.; Ferris, K. F. *J. Phys. Chem. B* **2001**, *105*, 6337–6346.
- (31) Sano, M.; Maruo, T.; Masuda, Y.; Yamatera, H. *Inorg. Chem.* **1984**, *23*, 4466–4469.
- (32) Rybak-Akimova, E. V.; Nazarenko, A. Y.; Chen, L.; Krieger, P. W.; Herrera, A. M.; Tarasov, V. V.; Robinson, P. D. *Inorg. Chim. Acta* **2001**, *324*, 1–15.
- (33) Su, C.-C.; Wu, C.-Y. *J. Coord. Chem.* **1994**, *33*, 1–14.
- (34) Inoue, M. B.; Navarro, R. E.; Inoue, M.; Fernando, Q. *Inorg. Chim. Acta* **1999**, *295*, 115–119.
- (35) De Santis, G.; Fabbri, L.; Manotti Lanfredi, A. M.; Pallavicini, P.; Perotti, A.; Ugozzoli, F.; Zema, M. *Inorg. Chem.* **1995**, *34*, 4529–4535.
- (36) Jiang, L.-J.; Luo, Q.-H.; Li, Q.-X.; Shen, M.-C.; Hu, H.-W. *Eur. J. Inorg. Chem.* **2002**, 664–670.
- (37) Benfatto, M.; D'Angelo, P.; Della Longa, S.; Pavel, N. V. *Phys. Rev. B: Condens. Matter* **2002**, *65*, 174205/174201–174205/174205.
- (38) Meltzer, A. D.; Tirrell, D. A.; Jones, A. A.; Inglefield, P. T.; Hedstrand, D. M.; Tomalia, D. A. *Macromolecules* **1992**, *25*, 4541–4548.
- (39) Aoi, K.; Motoda, A.; Ohno, M.; Tsutsumiuchi, K.; Okada, M.; Imae, T. *Polym. J. (Tokyo)* **1999**, *31*, 1071–1078.
- (40) Wilkins, R. G.; Lewis, J. *Modern coordination chemistry*; Interscience Publishers: New York, 1960.
- (41) Kau, L. S.; Spira-Solomon, D. J.; Penner-Hahn, J. E.; Hodgson, K. O.; Solomon, E. I. *J. Am. Chem. Soc.* **1987**, *109*, 6433–6442.
- (42) Kau, L. S.; Hodgson, K. O.; Solomon, E. I. *J. Am. Chem. Soc.* **1989**, *111*, 7103–7109.